2

Metal oxide-based electrode materials for supercapacitor applications

P.Y. Chan, S.R. Majid*

Centre for Ionics University of Malaya, University of Malaya, Kuala Lumpur, Malaysia
*Corresponding author

Outline

Introduction

The rapid growth in technology has led to the economic evolution from an agricultural-based to a more information-based economy. Consequently, it brings about the changes in social organisation and human life style. There are abundant of information emerged every day. In order to improve the efficiency in all aspects, it is essential for a digital citizen to manage information effectively. As one part of the society, the scientists have to keep up with the times and adopt the social responsibilities. Apart from the betterment of society, scientists also need to concern on the societal challenges. For example, the environmental pollution resulted from the civilization. This has prompted the development of alternative fuel vehicles such as electric vehicles. Although the very first electric vehicle invented between 1832-1839, there is only until the late of 1960s the electric vehicles re-attracted intensive attention due to the concern on environmental issues. As a result, the energy storage technology flourishes and grows. In addition to electric vehicles, the electrical devices we granted nowadays are the results of many years of research and development. In order to utilize the energy more efficiently, the energy storage technologies are vital in managing the power supply.
Battery is the most common energy storage device. It is favorable in many field applications due to its high-energy capacity. However, the insufficient power density of battery hinders it from the applications that require the large power impulses. Here is where the supercapacitor kicks in. Supercapacitor, or electrochemical capacitor, is well-known for its high power density compared to battery. It can works at high charge-discharge rates. A supercapacitor possesses energy density with several order of magnitude higher than conventional capacitor (hence the “super” prefix), **Fig. 2.1**. The supercapacitor can store charges through Faradaic and non-Faradaic reactions, which is then divided it into two kinds of supercapacitor. The research about supercapacitor is important because the hybrid power system derived from supercapacitor and battery can optimize the power performance of devices.

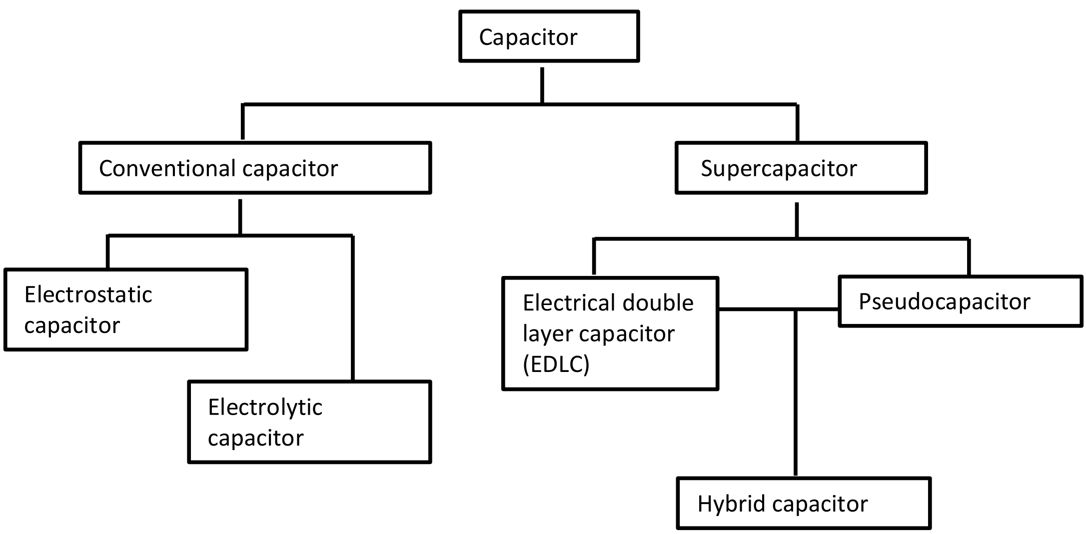

FIGURE 2.1
Categories of capacitor.

Electrostatic capacitor stores charge in the most literal way, that is, accumulates and holds electrical charges inside the electric field between the conductive electrodes (**Fig. 2.2 (a)**). The conductive electrodes are separated by a dielectric material or an insulator. The operating voltage of an electrostatic capacitor relies on the strength of the dielectric material. Electrostatic capacitor can offer capacitance less than 10 $\mu F\ g^{-1}$ and energy density not more than 0.1 $W\ h\ kg^{-1}$ (X. Zhao et al., 2011). Electrolytic capacitor has similar cell construction with electrostatic capacitor. The difference lies in the presence of conductive electrolyte spacer in an electrolytic capacitor (Sharma & Bhatti, 2010). The capacitance of an electrolytic capacitor is dependent on electrolyte inside the cell. Typically, it can achieve above 1μF. This allows it to be applicable in power supply and digital circuit. There are two types of electrolytic capacitor, determined by the materials used: one is aluminium electrolytic capacitor (**Fig. 2.2 (b)**) and second one is tantalum electrolytic capacitor.

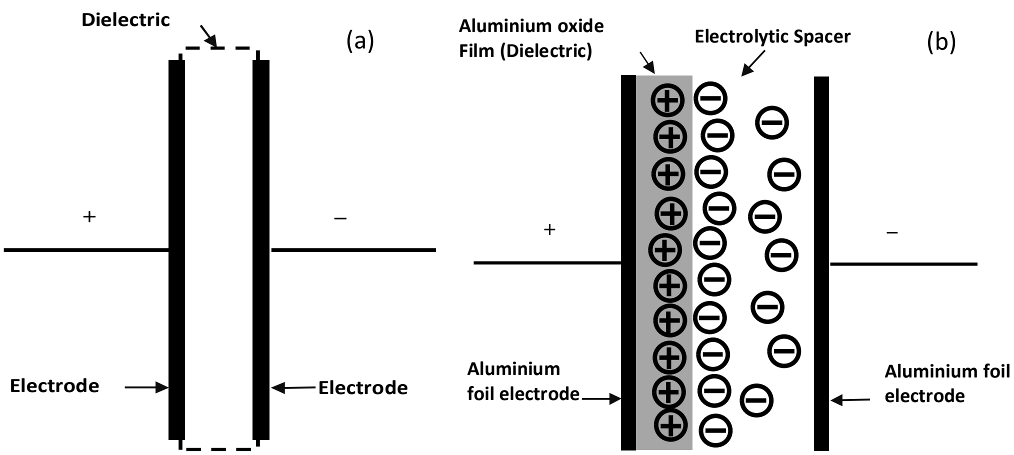

FIGURE 2.2
Configuration of (a) electrostatic capacitor and (b) aluminium electrolytic capacitor.

Principles of supercapacitor

The study on supercapacitor is divided into two areas that are mainly based on their energy storage mechanisms. The different energy storage mechanisms have categorized the supercapacitor into two groups. The first category is electric double layer capacitor (EDLC), which relies on the electrostatic storage of energy charge. There is no charge transferred at electrode/electrolyte interface. In other words, there is no electrochemical reactions occurred. The second category is pseudocapacitor which making use of charge transfer reactions for charge storage purpose.

Electric double layer capacitor (EDLC)

Electric double layer capacitor (EDLC) is the type of supercapacitor in which its performance mainly relies on the double layer capacitance. Although it stores charge in a similar way as a conventional capacitor, an EDLC can nevertheless store significantly more charge compared to conventional capacitor because: (a) the charge separation in the electrical double layer is very small, and (b) the surface area of electrode can be further enhanced in order to store more charges (Conway, 1999).

The energy storage mechanism is rapid due to the process that involves only the movement of ions from/to the electrode surface.

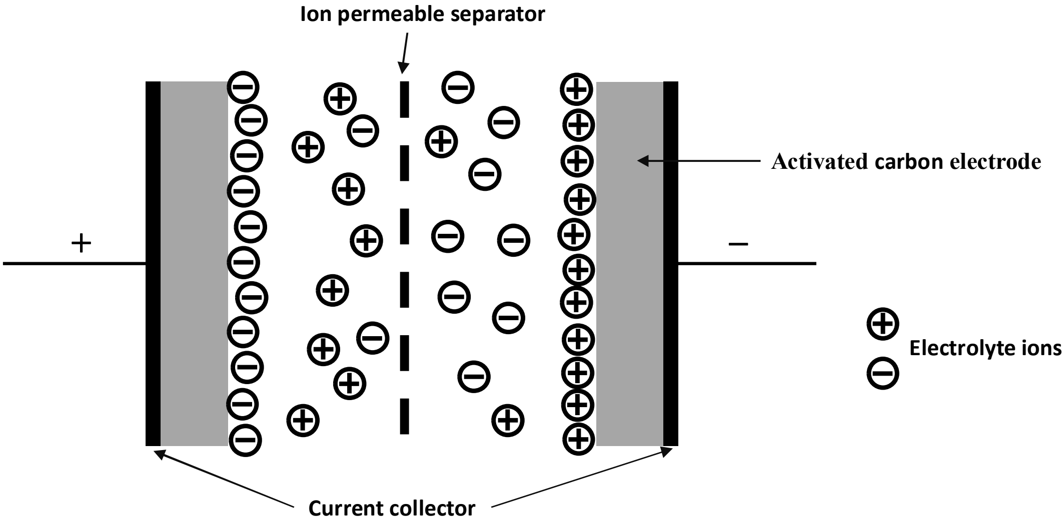

FIGURE 2.3
Configuration of electrical double layer capacitor (EDLC).

EDLC is the third generation evolution of capacitor after conventional capacitor and electrolytic capacitor. A basic configuration of EDLC is displayed in **Fig. 2.3**. In EDLC, each electrode/electrolyte interface acts like a capacitor. So, the complete cell can be considered as two capacitors in series. The cell capacitance (C_{cell}) for a symmetrical capacitor, with C1 and C2 that represent capacitances of first and second electrode, can be expressed as in **Eq. 2.1**. On the other hand, the double layer capacitance, C_{dl}, of single electrode is expressed as **Eq. 2.2**.

$$C_{cell} = \frac{1}{C_1} + \frac{1}{C_2}$$ **Equation 2.1**

$$C_{dl} = \frac{\varepsilon A}{4\Pi t}$$ **Equation 2.2**

where ε is the dielectric constant, *A* is the surface area of the electrode, and *t* is the thickness of double layer.
EDLC's dependence on electrostatic interaction for charge storage enabling it to sustain hundreds or thousands of cycles of charging and discharging. In reality, a capacitor encounters internal resistance contributed from the electrode, current collector and dielectric. In order to take into account of this, a voltage drop is introduced and the resistances are designated as equivalent series resistance (R_{ESR}). Thus, the maximum electrical power (P), which is the maximum rate of energy transfer, can be determined (**Eq. 2.3**). It is important to specify that the specific capacitance estimated is either from single-electrode measurement or two-electrode configuration in order to get rid of confusion on the real capability of the electrode material.

$$P_{max} = \frac{V^2}{4R_{ESR}}$$ **Equation 2.3**

Due to the high surface area, high conductivity, and high temperature stability, the carbon materials such as activated carbon, graphene and carbon nanotube have been widely studied and applied as the electrode material for EDLC (Pandolfo & Hollenkamp, 2006). Although the charge storage on carbon materials-based electrode is mainly capacitive, there are also contributions from surface functional groups which give rise to pseudocapacitance (Kötz & Carlen, 2000). The pseudocapacitance can be related with the oxidative treatment and increases with the extent of oxygen treatment (Hsieh & Teng, 2002). However, the corresponding internal resistance and leakage current are also higher.

Pseudocapacitor

Previous studies about EDLC using carbon electrode had discovered the participation of pseudocapacitance in the charge storage processes. The contribution of pseudocapacitance to the total capacitance is small but significant. It is caused by the partial charge transfer reactions during chemisorption processes. The main difference between pseudocapacitance and double layer capacitance lies in the charge storage mechanism, that is, the charge storage originates from the electron transfer reactions for pseudocapacitance while double layer capacitance depends on the pure accumulation of electrolyte ions on the electrode surface.
The term of 'pseudocapacitive' is more appropriate to be used to describe a single electrode material rather than a system (Brousse et al., 2015). This is because we cannot speculate the processes occurred inside a system solely based on the macroscopic behaviour. In general, pseudocapacitance arises when reversible redox reactions take place at the interface of electrode/electrolyte (Augustyn et al., 2014). The pseudocapacitive electrode material exhibits electrochemical feature of a capacitive electrode (Brousse et al., 2015; Conway, 1999). In other words, the charge stored in these pseudocapacitive electrode materials responds linearly to the potential applied. There are three kinds of pseudocapacitive mechanisms: underpotential deposition, redox pseudocapacitance, and intercalation pseudocapacitance (Conway, 1999). Underpotential deposition refers to the formation of monolayer resulted by the adsorption of metal ions on the metal electrode's surface. Redox pseudocapacitance is the product of electrochemical adsorption with charge transfer. Intercalation pseudocapacitance refers to the capacitance contributed by the Faradaic charge transfer reactions tooking place along with the intercalation of ions into layers or tunnels of a redox active material without crystallographic phase change.

Electrode materials for pseudocapacitor

The electrode materials that can be utilised for supercapacitor are carbon material, metal oxide, and conducting polymer. The carbon materials such as activated carbon, carbon nanotubes (CNTs), multi-walled carbon nanotubes (MWCNTs), single-walled carbon nanotubes (SWCNTs), and graphene are usually employed as electrode for EDLC as they exhibit capacitive behaviour. On the other hand, metal oxide especially transition metal oxide and conducting polymers are redox materials. Hence, they are used as electrode material for pseudocapacitor.

Nevertheless, we will focus on the electrochemical performance of metal oxide-based electrode material.

Ruthenium oxide

In 1971, the study of RuO_2 in H_2SO_4 has firstly uncovered the alternative charge storage mechanism through redox reactions (Trasatti & Buzzanca, 1971). Since then, tremendous effort has been made on ruthenium oxide in order to comprehend the pseudocapacitive behaviour. Before being the well-known transition metal oxide studied for pseudocapacitor, the ruthenium oxide also being studied as chlorine and oxygen evolving anodes due to its electrocatalytic properties (L. D. Burke & Healy, 1981; L. D. Burke & McCarthy, 1984; Laurence D. Burke & Murphy, 1980; Melsheimer & Ziegler, 1988; Trasatti, 1987). Both crystalline and hydrous forms of ruthenium oxide exhibit good electrochemical behaviors. In 1995, Zheng J.P. et al. had attributed the high specific capacitance (720 F g^{-1}) achieved by hydrous ruthenium oxide to the hydrous region within the nanoparticles (Zheng & Jow, 1995). In addition, there are another three contributions for the electrochemical performance of hydrous ruthenium oxide proposed: (i) electron hopping between electrode material and current collector, (ii) electron hopping between particles, and (iii) electron hopping within $RuO_x{\cdot}n$H2O.
As one of the metal in platinum group, ruthenium (Ru) appears to be precious and expensive. The high-cost of this material has hindered it from commercial application. However, its excellent electrochemical properties never impede the further exploration on the ruthenium oxide. Though many studies have emphasized on other possible transition metal oxides, the reports on ruthenium oxide have also being published at the same time. As an alternative, researchers direct the preparation methods to be more productive and high-yielding. From thermal decomposition, which is a common technique used to fabricate RuO_2, the methodology has been developed to deposition, sol-gel, hydrothermal, and inkjet printing.

TABLE 2.1
Literature review on RuO_2-based electrode.

No.	Preparation method	Film properties	Specific capacitance (F g^{-1})	Reference
1	Hydrothermal	Hydrous RuO_2 with multi-walled carbon nanotubes (MWCNT)	1585	(Chaitra et al., 2016)
2	Facile template method	Hydrous RuO_2 nanotubes	745	(Xu Wu et al., 2015)
3	Microwave-hydrothermal	One dimensional $RuO_2{\cdot}1.84H_2O$	511	(Kim et al., 2015)
4	Laser scribing method	Graphene/RuO_2 nanocomposite	1139	(Hwang et al., 2015)
5	Hydrothermal	RuO_2/graphene	528	(Leng et al., 2015)
6	Solution phase assembly	RuO_2/graphene	479	(Deng et al., 2014a)
7	Successive ionic layer adsorption and reaction (SILAR)	PANI-RuO_2	664	(Deshmukh et al., 2014)
8	Hydrothermal	RuO_2-reduced graphene oxide (RGO)	521	(Shen et al., 2013)

9	Electropolymerisation and redox deposition	Nanoscopic RuO_2/ PANI/ carbon double-shelled hollow spheres	531	(D. Zhao et al., 2012)
10	Chemical bath deposition (CBD)	RuO_2 thin film	73	(Patil et al., 2011)
11	Inkjet printing	Single-walled carbon nanotube/RuO_2 nanowire	138	(P. Chen et al., 2010)
12	Sol-gel and low temperature annealing	Hydrous RuO_2/graphene with particle-attached layered structure	570	(Z.-S. Wu et al., 2010)
13	Sacrificial template method	Tubular $RuO_x \cdot nH_2O$	860	(Jintao Zhang et al., 2010)
14	Anodic deposition	Porous RuO_2	276	(Mondal & Munichandraiah, 2008)
15	Modified chemical bath deposition (M-CBD)	RuO_2 thin film	50	(Patake & Lokhande, 2008)
16	Cathodic deposition	RuO_2 thin film	650	(Patake et al., 2009)

Table 2.1 shows variety of preparation methods and the corresponding specific capacitances achieved by the RuO_2-based electrodes. The deposition techniques presented in **Table 2.1** includes cathodic deposition, anodic deposition, chemical bath deposition, redox deposition, and successive ionic layer adsorption and reaction (SILAR). The deposition methods are considered simple, cost-effective, and advantageous that the desired film can be deposited directly on the substrate. Generally, the deposited films are amorphous in nature with porous structure. By comparing the specific capacitances achieved by the electrode materials consisted only the ruthenium oxide, the values range from 50 to 650 F g^{-1}. The higher specific capacitance was obtained by RuO_2 electrode prepared through cathodic deposition method (Patake et al., 2009). This report has highlighted the significance of porosity on the electrochemical performance. The RuO_2 film fabricated using anodic deposition method also presented a good specific capacitance of 276 F g^{-1} (Mondal & Munichandraiah, 2008). The authors attributed the contribution to the higher porosity produced at higher current density during deposition. The current density values examined in this study allowed the simultaneous deposition of RuO_2 along with oxygen evolution reaction (OER) to occur. The OER was found to be helpful as it improved the porosity of the film. On the other hand, the RuO_2 thin films prepared using chemical bath deposition (CBD) achieved relatively lower value of specific capacitances. In CBD, the deposition takes place on the substrate that immersed in the dilute chemical bath made up of anionic and cationic precursors. The deposition occurs together with the formation of precipitate in the bulk solution which is unfavourable (Pathan & Lokhande, 2004). The precipitation indicates the unnecessary loss of material which can impact on the electrochemical performance of electrode material. Thus, this technique has been modified and developed to be successive ionic layer adsorption and reaction (SILAR). The specific capacitance obtained by the RuO_2 electrode prepared using SILAR method also shown to be relatively higher (Deshmukh et al., 2012). In addition, the SILAR method is usually employed in solar cell preparation.

Alternative approach to reduce RuO_2 effective cost is to integrating RuO_2 with other materials. As a pseudocapacitive material, RuO_2 turns out to be an attractive material to combine with carbon material that is suffered with relatively lower capacitance. Carbon materials can act as backbone for RuO_2 particles, offer the conducting pathway for electrolyte ion, and provide higher surface area for charge storage. The uniform distribution of RuO_2 particles can be easily obtained through incorporation with the carbon material irrespective of the preparation methods (Chaitra et al., 2016; Hwang et al., 2015; X. Wang et al., 2015; Z.-S. Wu et al., 2010). The synergistic effect of combining non-Faradaic and Faradaic materials is remarkable. The specific capacitance is enhanced significantly. For instance, the specific capacitance value is boosted from 604 to 1585 F g^{-1} when RuO_2 is combined with MWCNT (Chaitra et al., 2016). Although the BET surface area of composite is lower than those of individual RuO_2 and MWCNT, the pore volume and average pore diameter are higher compared to individual RuO_2. Since the RuO_2 is accountable for the charge storage, the enhanced pore volume and average pore diameter are indeed favourable for better electrochemical performance. On the other hand, RuO_2 nanoparticles can improve the attachment of CNT on the substrate and thus ameliorate the ionic conductivity (X. Wang et al., 2015). Graphene, as a carbon material that has good conductivity (2000 S cm^{-1}), is another material that is widely studied as composite with RuO_2. The RuO_2-graphene composites usually exhibit good specific capacitance values that vary from 479 to 1139 F g^{-1} (Deng et al., 2014b; Hwang et al., 2015; Z.-S. Wu et al., 2010).

Laser scribing method has been employed to synthesize RuO2/graphene (Hwang et al., 2015). The RuO_2 nanoparticles were dispersed well on graphene sheet. The uniform dispersion of RuO_2 on graphene allows the more efficient ionic and electronic transportations. This highly porous graphene with RuO_2 nanoparticles composite has demonstrated a high specific capacitance of 1139 F g^{-1}. The Van der Waals attractions between graphene sheets that can bring to restacking is a challenge to overcome when the graphene is employed. Hence, an optimizing condition is required to prepare RuO_2/graphene composite. Sodium hydroxide (NaOH) was found to be a better precipitant compared to ammonium carbonate ($(NH_4)_3CO_2$) and carbamide or urea ($Co(NH_2)_2$) when the hydrothermal method was used (Leng et al., 2015). Different precipitants produced various morphologies. $((NH_4)_3CO_2$ has led to the formation of inhomogeneous structure with less pores while $Co(NH_2)_2$ produced more homogenous structure with spherical particles. On the other hand, NaOH formed a veil-like morphology. The electrochemical test has shown the better performance of RuO_2/graphene composite produced with the aid of NaOH, where the specific capacitance achieved was 528 F g^{-1}. Although the RuO_2/graphene formed without precipitant also exhibited veil-like morphology, its specific capacitance was only 358 F g^{-1}. This shows the importance of a suitable precipitant for hydrothermal method.

Conducting polymer is another material that can be incorporated with RuO_2. For instance, RuO_2/PANI composite can be fabricated using successive ionic layer adsorption and reaction (SILAR) (Deshmukh et al., 2014). The RuO_2 nanoparticles were grown on the nanofibers of PANI. The combination of RuO_2 with PANI has led to the production of more porous structure and thus higher active surface area. In order to enhance the backbone for electron transportation, carbon material is again a good candidate to integrate with RuO_2/PANI. A double-shelled carbon sphere could combine first with PANI to form a strong foundation for RuO_2 (D. Zhao et al., 2012). However, the specific capacitance achieved was 531 F g^{-1}. It is lower compared to the RuO_2/PANI prepared using SILAR method, which is 664 F g^{-1}. The difference can be attributed to the morphologies formed between them. It is well-known that higher porosity can optimize the ionic and electronic transportations. The RuO_2/PANI was observed to have more porous structure. Thus, there is no doubt that RuO_2/PANI could achieve higher specific capacitance with its higher porosity structure. From here, the electrochemical performance is again shown to be morphology dependent.

A composite electrode prepared using repetitive impregnations procedure has achieved 1000 F g^{-1} of specific capacitance (Barranco et al., 2009). It consisted of ruthenium oxide deposited on amorphous carbon nanofibers. The composite electrode showed high porosity of 450 m^2 g^{-1}. The amorphous carbon nanofibers acted as the backbone for ruthenium oxide and so for charge storage. The repetitive impregnation method has been compared with impregnation involved $Ru(acac)_3$ vapour (Pico et al., 2009). The relationship between the particle size of $RuO_2{\cdot}nH_2O$ and the pore size of carbon support was also investigated. The repetitive impregnations of carbon with $RuCl_3{\cdot}0.5H_2O$ was found to produce particles with less crystallinity. In other words, the electrode prepared using this method could achieve higher specific capacitance. Another finding of them revealed the smaller size of particles compared to the pore size of carbon support that could lead to higher specific capacitance.

Manganese oxide

The manganese (Mn) is abundant in nature. It appears in the form of ore and native metallic nodules. As a transition metal oxide, manganese oxide has seven oxidation states: Mn(0), Mn(II), Mn(III), Mn(IV), Mn(V), Mn(VI), and Mn(VII) (Messaoudi et al., 2001). Similar to ruthenium oxide, the water content in manganese oxide is vital in its electrochemical reactivity and thermodynamic stability of each manganese oxide phases (Desai et al., 1985). Due to this reason, sol-gel method is usually employed to prepare manganese oxide film. **Table 2.2** displays the film properties and specific capacitance achieved by manganese oxide-based film prepared using different methods.

TABLE 2.2
Literature review on MnO_x-based electrode.

No.	Preparation method	Film properties	Specific capacitance ($F\ g^{-1}$)	Reference
1	Anodic deposition	Manganese oxide nanostructure grown on nanoporous gold film	432	(Shi et al., 2017)
2	Electrodeposition	Co_3O_4–MnO_2–NiO nanotubes	2525	(Singh et al., 2016)
3	Spray pyrolysis	Mn_3O_4 thin film	394	(Yadav et al., 2016)
4	Urea hydrolysis	Nickel-manganese layered double hydroxide	1511	(Guo et al., 2016)
5	Electrodeposition	Cobalt-manganese layered double hydroxide	1062	(Jagadale et al., 2016)
6	Sacrificial reaction	Manganese oxide decorated graphene nanosheets	280	(Unnikrishnan et al., 2016)
7	Anodic deposition	Mn-Ni oxide	250	(Tahmasebi et al., 2016)
8	Sol-gel method	Manganese oxide/multi-walled carbon nanotubes (MWCNT)	339	(S.-H. Chen et al., 2016)
9	Sol-gel method	Manganese oxide film	360	(Sarkar et al., 2015)
10	Hydrothermal	Mn_3O_4/graphene	367	(H.-M. Lee et al., 2015)

11	Hydrothermal	$Ni(OH)_2/MnO_2$/RGO	1985	(H. Chen et al., 2014)
12	Electrospinning	Carbon nanofiber/MnO_2 core-shell tubular structure	237	(Hong et al., 2014)
13	Electrospinning	Carbon nanofiber/MnO_2	311	(Zhi et al., 2012)
14	Hydrothermal	Nickel-manganese oxide	284	(C.-H. Wu et al., 2012)
15	Cathodic deposition	Manganese oxide thin film	365	(Liu et al., 2010)

From **Table 2.2**, the specific capacitance of MnO_x thin film estimated from galvanostatic charge-discharge test ranges from 360 to 394 F g^{-1} regardless of the preparation methods i.e. spray pyrolysis, sol-gel method, and cathodic deposition (Liu et al., 2010; Sarkar et al., 2015; Yadav et al., 2016). It is important to remember that, thin film is more favourable for MnO_x in order to achieve better electrochemical performance (Broughton & Brett, 2004; Pang et al., 2000; Toupin et al., 2004). As there is only surface and sub-surface of MnO_x film participate in charge storage process, thicker film will create higher dead volume that hinders the ionic and electronic transportation. In addition, thick film causes significant degradation in electrochemical performance during cycling (Pang et al., 2000). Compare to thick film, thin film offers a better coating on substrate that eventually minimises the resistance in ionic transportation. The substrate used plays an influential role in determining the electrochemical performance. A conductive network can enhance the capacitance (S.-H. Chen et al., 2016). The most common conductive network employed is the carbon material. An optimal amount of carbon material such as MWCNT aids the formation of porous structure and preserves the connectivity within the network (S.-H. Chen et al., 2016; S. W. Lee et al., 2010). Graphene is another excellent carbon material to incorporate with MnO_x. The MnO_x particles anchored on the graphene sheets can prevent the stacking of graphene sheets while graphene sheets prohibit the agglomeration of MnO_x particles.

Aside from the carbon materials, the addition of different materials can also improve the electrochemical performance of MnO_x film by forming different beneficial morphologies for ionic transportation. The addition of nickel has caused a rod-like structure turned to plate-like and decline in particle size (C.-H. Wu et al., 2012). The composite comprised of cobalt and manganese oxide showed a three dimensional network with nanoscale fibers (Chang et al., 2008). The ternary composite is another widely studied material. An excellent electrochemical performance (2525 F g^{-1}) has been achieved by Co_3O_4–MnO_2–NiO ternary hybrid nanotubes (Singh et al., 2016). It can be attributed to the well-aligned arrays of nanotubes formed which allows the easy penetration of electrolyte ions. On the other hand, $Ni(OH)_2/MnO_2$/RGO prepared using hydrothermal method also exhibited 1985 F g^{-1} of specific capacitance (H. Chen et al., 2014). The charge storage was facilitated by the porous flowerlike structure formed.

A layered double hydroxide (LDH) is an anionic clay represented by the formula $[M^{2+}{}_{1-x}\, M^{3+}{}_{x}\, (OH)_2]^{x+}\, A^{z-}{}_{x/z} \cdot mH_2O$ where M^{2+} is a divalent cation, M^{3+} is a trivalent cation, and A^{z-} serves as any organic or inorganic anion (Cavani et al., 1991). It can be prepared using simple electrodeposition method or urea hydrolysis. Both LDHs show high specific capacitances in the range of 1000 F g^{-1} with different morphologies obtained. Electrodeposited CoMn-LDH appeared as hexagonal platelets like morphology while NiMn-LDH synthesised using urea hydrolysis method showed nanosheets structure (Guo et al., 2016; Jagadale et al., 2016). Their cycling stabilities were excellent as well. CoMn-LDH retained around 65% after 5000 cycles while NiMn-LDH preserved more than 90% after 3000 cycles. The similarity between these two LDHs is the employment of nickel foam as the substrate. The nickel foam is well-known for its good mechanical strength which offers a strong support for LDH formed. Besides nickel foam, gold substrate especially nanoporous gold substrate also acts as a good substrate. The manganese oxide film deposited on the nanoporous gold substrate was grown with porous and aggregated nanosheets structure (Shi et al., 2017). The film deposited at the same current density but using gold substrate was observed to have continuous structure with equiaxed particles. The nanoporous gold substrate has contributed to the electrochemical performance of the manganese oxide film by providing a higher specific surface area than gold substrate, hence higher specific capacitance was expected for former substrate.

Nickel oxide

Due to its environmental friendliness and natural abundance, NiO_x is one of the potential electrode materials to be used in supercapacitor. It has multiple oxidation states which favour fast redox reactions and thus can contribute in charge storage processes. Aside from supercapacitor, NiO_x has been widely studied as electrode material for other applications such as battery, fuel cell, gas sensors, and electrochromic films (Mamak et al., 2001; Michalak et al., 1999; Poizot et al., 2000; C. Wang et al., 2015). Although NiO_x has a high theoretical specific capacitance (3750 F g^{-1}), it is poor in electronic conductivity. It cannot sustain in repetitive charge-discharge processes because it experiences volume expansion that can destruct the active materials and damage the electrical contact (Zhuo et al., 2013).

Table 2.3 shows some finding of past studies for NiO_x-based electrode. Even without the additional material, nickel oxide was found to exhibit high specific capacitance of 1337 F g^{-1} (Pei et al., 2016). Solvent was realised to be important in determining the morphology and electrochemical performance of NiO_x. The introduction of ethanol into the deionized water has changed the morphology of NiO_x gradually. The nanoflakes structure became more fragmented with the higher volume ratio of ethanol to water.

The nickel foam and carbon cloth are always employed as substrate nowadays due to their high electrical conductivity and strong mechanical property. The NiO on nickel foam using hydrothermal method showed specific capacitance of 674 F g^{-1} (Huang et al., 2014). On the other hand, the carbon cloth supported NiO_x synthesized using chemical bath deposition method displayed 660 F g^{-1} (Zhang et al., 2014). Both films exhibited high cycling stability. The NiO on nickel foam retained around 93% after 5000 cycles while the one deposited on carbon cloth has successfully kept 82% from its initial capacitance after 4000 cycles. The morphologies formed between them are similar: nanosheets/nanoflakes. Hence, the slight difference in electrochemical performance can attribute to the substrate used.

Chemical bath deposition can also be used to prepare NiO_x-based composite. For example, nickel-cobalt oxyhydroxide on carbon nanotubes ((Ni, Co) OOH/CNT) has been successfully synthesized using this method (Li et al., 2015). Compared to the electrode consisted only nickel oxide, this electrode exhibited a good specific capacitance of 940 F g^{-1}, which is higher than the carbon cloth supported nickel oxide prepared using same method (660 F g^{-1}). This (Ni, Co) OOH/CNT possessed a unique core shell structure. The (Ni, Co) OOH nanoflakes are densely attached on the carbon nanotubes. This special structure allows the easy penetration of electrolyte ions thus lead to relatively higher specific capacitance.

By using simple electrodeposition technique, a good specific capacitance of 950 F g^{-1} can be achieved (B. Zhao et al., 2016). The high specific capacitance is contributed by the morphology formed and the substrate used which is nickel foam. Graphene acts as the strong binder between nickel oxide and nickel foam that avoids the exfoliation of nickel oxide from substrate. When nickel oxide directly electrodeposited on substrate, it may performs not as good as those deposited with additional materials. For example, the NiO_x deposited on carbon nanofoam only shows 150 F g^{-1} (Della Noce et al., 2016). The additional material is not only acting as the binder, it can also guide the formation of desired morphology. Other than chemical bath deposition, hydrothermal, and electrodeposition, the solvothermal is also a good method for electrode preparation. $Ni(OH)_2$/RGO composite prepared using solvothermal method exhibited 1886 F g^{-1} (Zang et al., 2017). The composite has an interconnected porous structure. When PANI was added into nickel oxide/graphene composite, the surface of composite was covered uniformly by PANI without changing the morphology significantly (Xinming Wu et al., 2016).

Binary oxide of $NiCo_2O_4$ has been reported with its excellent electrochemical performance and thus receives worldwide attention. It can be prepared using simple technique such as co-precipitation, or hydrolysis process. $NiCo_2O_4$/graphene oxide composite fabricated using co-precipitation method exhibited 1211 F g^{-1} (Y. Xu et al., 2016). With the aid of sodium dodecyl sulfate (SDS), the morphology of $NiCo_2O_4$/graphene oxide transformed from mesoporous structure to flowerlike structure. On the other hand, $NiCo_2O_4$/SWCNT prepared using controlled hydrolysis method showed specific capacitance of 1642 F g^{-1} (Wang et al., 2012). The water: ethanol ratio was adjusted in order to find out the best composition of solvent for $NiCo_2O_4$/SWCNT electrode. Different water/ethanol ratio led to different morphologies formed. The water: ethanol ratio of 1: 4 was found out to be the optimal condition to produce the electrode with better electrochemical performance. The well-separated nanowires structure formed is believed to be contributed to the charge transfer reactions.

TABLE 2.3

Literature review on NiO_x-based electrode.

No.	Preparation method	Film properties	Specific capacitance (F g^{-1})	Reference
1	Solvothermal	$Ni(OH)_2$/RGO	1886 F g^{-1}	(Zang et al., 2017)
2	Hydrothermal and *in situ* chemical oxidative polymerization	Nickel oxide coated graphene/PANI	1409 F g^{-1}	(Xinming Wu et al., 2016)
3	Microwave	Nitrogen-doped mesoporous carbon/nickel cobalt layered double hydroxide	2498 F g^{-1}	(J. Xu et al., 2016)
4	Co-precipitation	Nickel cobalt oxide/graphene oxide	1211 F g^{-1}	(Y. Xu et al., 2016)
5	Hydrothermal	NiO nanomaterial	1337 F g^{-1}	(Pei et al., 2016)
6	Electrodeposition	NiO/RGO	950 F g^{-1}	(B. Zhao et al., 2016)
7	Anodic deposition	NiO_x on carbon nanofoam	150 F g^{-1}	(Della Noce et al., 2016)
8	Alternating voltage approach	Nickel oxide quantum dots embedded with graphene	1181 F g^{-1}	(Jing et al., 2015)

9	Chemical bath deposition	Nickel-cobalt oxyhydroxide/oxide on carbon nanotubes	940 F g^{-1}	(Li et al., 2015)
10	Chemical bath deposition	NiO nanoflake/carbon cloth	660 F g^{-1}	(Zhang et al., 2014)
11	Hydrothermal	NiO nanosheets on Ni foam	674 F g^{-1}	(Huang et al., 2014)
12	Electrodeposition	Manganese-nickel oxide film on graphite sheet	424 F g^{-1}	(H.-M. Lee et al., 2014)
13	Controlled hydrolysis process	$NiCo_2O_4$-single wall carbon nanotubes (SWCNT)	1642 F g^{-1}	(Wang et al., 2012)
14	Chemical precipitation method	Porous nickel oxide/mesoporous carbon	2570 F g^{-1}	(Jing Zhang et al., 2010)

Conclusion

Metal oxide appears to be an attractive electrode material for supercapacitor application. The major factors that affect the electrochemical performance of metal oxide-based electrode are: (a) various structures formed by different preparation methods, (b) synergistic effect contributed by a variety combination of different materials, and (c) different experimental conditions employed. The charge storage processes for different additions of materials are complicated and not our focus of study here. However, further understanding on the charge storage mechanism of various combinations of materials aids in the enhancement of the electrochemical performance of the supercapacitor electrode.

Acknowledgements

The authors acknowledge the University of Malaya for providing financial support through the project FP008-2013B and BKS030-2017.

References

1. Augustyn, V., Simon, P., & Dunn, B. (2014). Pseudocapacitive oxide materials for high-rate electrochemical energy storage. *Energy Environ. Sci., 7*(5), 1597-1614
2. Barranco, V., Pico, F., Ibañez, J., Lillo-Rodenas, M. A., Linares-Solano, A., Kimura, M., . . . Rojo, J. M. (2009). Amorphous carbon nanofibres inducing high specific capacitance of deposited hydrous ruthenium oxide. *Electrochimica Acta, 54*(28), 7452-7457
3. Broughton, J. N., & Brett, M. J. (2004). Investigation of thin sputtered Mn films for electrochemical capacitors. *Electrochimica Acta, 49*(25), 4439-4446
4. Brousse, T., Bélanger, D., & Long, J. W. (2015). To Be or Not To Be Pseudocapacitive? *Journal of The Electrochemical Society, 162*(5), A5185-A5189

5. Burke, L. D., & Healy, J. F. (1981). The importance of reactive surface groups with regard to the electrocatalytic behaviour of oxide (Especially RuO2) anodes. *Journal of Electroanalytical Chemistry and Interfacial Electrochemistry, 124*(1), 327-332
6. Burke, L. D., & McCarthy, M. (1984). Oxygen gas evolution at, and deterioration of, RuO2/ZrO2-coated titanium anodes at elevated temperature in strong base. *Electrochimica Acta, 29*(2), 211-216
7. Burke, L. D., & Murphy, O. J. (1980). The electrochemical behaviour of RuO2-based mixed-oxide anodes in base. *Journal of Electroanalytical Chemistry and Interfacial Electrochemistry, 109*(1), 199-212
8. Cavani, F., Trifirò, F., & Vaccari, A. (1991). Hydrotalcite-type anionic clays: Preparation, properties and applications. *Catalysis Today, 11*(2), 173-301
9. Chaitra, K., Sivaraman, P., Vinny, R. T., Bhatta, U. M., Nagaraju, N., & Kathyayini, N. (2016). High energy density performance of hydrothermally produced hydrous ruthenium oxide/multiwalled carbon nanotubes composite: Design of an asymmetric supercapacitor with excellent cycle life. *Journal of Energy Chemistry, 25*(4), 627-635
10. Chang, J.-K., Lee, M.-T., Huang, C.-H., & Tsai, W.-T. (2008). Physicochemical properties and electrochemical behavior of binary manganese–cobalt oxide electrodes for supercapacitor applications. *Mater. Chem. Phys., 108*(1), 124-131
11. Chen, H., Zhou, S., & Wu, L. (2014). Porous Nickel Hydroxide–Manganese Dioxide-Reduced Graphene Oxide Ternary Hybrid Spheres as Excellent Supercapacitor Electrode Materials. *ACS Applied Materials & Interfaces, 6*(11), 8621-8630
12. Chen, P., Chen, H., Qiu, J., & Zhou, C. (2010). Inkjet printing of single-walled carbon nanotube/RuO2 nanowire supercapacitors on cloth fabrics and flexible substrates. *Nano Research, 3*(8), 594-603
13. Chen, S.-H., Wu, C.-H., Fang, A., & Lin, C.-K. (2016). Effects of adding different morphological carbon nanomaterials on supercapacitive performance of sol–gel manganese oxide films. *Ceramics International, 42*(4), 4797-4805
14. Conway, B. E. (1999). *Electrochemical Supercapacitors: Scientific Fundamentals and Technological Applications*: Springer US.
15. Della Noce, R., Eugenio, S., Boudard, M., Rapenne, L., Silva, T. M., Carmezim, M. J., . . . Montemor, M. F. (2016). One-step process to form a nickel-based/carbon nanofoam composite supercapacitor electrode using Na2SO4 as an eco-friendly electrolyte. *RSC Advances, 6*(19), 15920-15928
16. Deng, L., Wang, J., Zhu, G., Kang, L., Hao, Z., Lei, Z., . . . Liu, Z.-H. (2014a). RuO2/graphene hybrid material for high performance electrochemical capacitor. *Journal of Power Sources, 248*, 407-415
17. Desai, B. D., Fernandes, J. B., & Dalal, V. N. K. (1985). Manganese dioxide — a review of a battery chemical Part II. Solid state and electrochemical properties of manganese dioxides. *Journal of Power Sources, 16*(1), 1-43
18. Deshmukh, P. R., Patil, S. V., Bulakhe, R. N., Sartale, S. D., & Lokhande, C. D. (2014). Inexpensive synthesis route of porous polyaniline–ruthenium oxide composite for supercapacitor application. *Chemical Engineering Journal, 257*, 82-89
19. Deshmukh, P. R., Pusawale, S. N., Jagadale, A. D., & Lokhande, C. D. (2012). Supercapacitive performance of hydrous ruthenium oxide (RuO2·nH2O) thin films deposited by SILAR method. *Journal of Materials Science, 47*(3), 1546-1553

20. Guo, X. L., Liu, X. Y., Hao, X. D., Zhu, S. J., Dong, F., Wen, Z. Q., & Zhang, Y. X. (2016). Nickel-Manganese Layered Double Hydroxide Nanosheets Supported on Nickel Foam for High-performance Supercapacitor Electrode Materials. *Electrochimica Acta, 194*, 179-186
21. Hong, S., Lee, S., & Paik, U. (2014). Core-Shell Tubular Nanostructured Electrode of Hollow Carbon Nanofiber/Manganese Oxide for Electrochemical Capacitors. *Electrochimica Acta, 141*, 39-44
22. Hsieh, C.-T., & Teng, H. (2002). Influence of oxygen treatment on electric double-layer capacitance of activated carbon fabrics. *Carbon, 40*(5), 667-674
23. Huang, M., Li, F., Ji, J. Y., Zhang, Y. X., Zhao, X. L., & Gao, X. (2014). Facile synthesis of single-crystalline NiO nanosheet arrays on Ni foam for high-performance supercapacitors. *CrystEngComm, 16*(14), 2878-2884
24. Hwang, J. Y., El-Kady, M. F., Wang, Y., Wang, L., Shao, Y., Marsh, K., . . . Kaner, R. B. (2015). Direct preparation and processing of graphene/RuO2 nanocomposite electrodes for high-performance capacitive energy storage. *Nano Energy, 18*, 57-70
25. Jagadale, A. D., Guan, G., Li, X., Du, X., Ma, X., Hao, X., & Abudula, A. (2016). Ultrathin nanoflakes of cobalt–manganese layered double hydroxide with high reversibility for asymmetric supercapacitor. *Journal of Power Sources, 306*, 526-534
26. Jing, M., Wang, C., Hou, H., Wu, Z., Zhu, Y., Yang, Y., . . . Ji, X. (2015). Ultrafine nickel oxide quantum dots enbedded with few-layer exfoliative graphene for an asymmetric supercapacitor: Enhanced capacitances by alternating voltage. *Journal of Power Sources, 298*, 241-248
27. Kim, J.-Y., Kim, K.-H., Kim, H.-K., Park, S.-H., Roh, K. C., & Kim, K.-B. (2015). Template-Free Synthesis of Ruthenium Oxide Nanotubes for High-Performance Electrochemical Capacitors. *ACS Applied Materials & Interfaces, 7*(30), 16686-16693
28. Kötz, R., & Carlen, M. (2000). Principles and applications of electrochemical capacitors. *Electrochimica Acta, 45*(15–16), 2483-2498
29. Lee, H.-M., Jeong, G. H., Kang, D. W., Kim, S.-W., & Kim, C.-K. (2015). Direct and environmentally benign synthesis of manganese oxide/graphene composites from graphite for electrochemical capacitors. *Journal of Power Sources, 281*, 44-48
30. Lee, H.-M., Lee, K., & Kim, C.-K. (2014). Electrodeposition of manganese-nickel oxide films on a graphite sheet for electrochemical capacitor applications. *Materials, 7*(1), 265-274
31. Lee, S. W., Kim, J., Chen, S., Hammond, P. T., & Shao-Horn, Y. (2010). Carbon Nanotube/Manganese Oxide Ultrathin Film Electrodes for Electrochemical Capacitors. *ACS Nano, 4*(7), 3889-3896
32. Leng, X., Zou, J., Xiong, X., & He, H. (2015). Electrochemical capacitive behavior of RuO2/graphene composites prepared under various precipitation conditions. *Journal of Alloys and Compounds, 653*, 577-584
33. Li, M., Cheng, J. P., Liu, F., & Zhang, X. B. (2015). In situ growth of nickel-cobalt oxyhydroxide/oxide on carbon nanotubes for high performance supercapacitors. *Electrochimica Acta, 178*, 439-446
34. Liu, J., Essner, J., & Li, J. (2010). Hybrid Supercapacitor Based on Coaxially Coated Manganese Oxide on Vertically Aligned Carbon Nanofiber Arrays. *Chem. Mater., 22*(17), 5022-5030
35. Mamak, M., Coombs, N., & Ozin, G. A. (2001). Mesoporous Nickel−Yttria−Zirconia Fuel Cell Materials. *Chem. Mater., 13*(10), 3564-3570

36. Melsheimer, J., & Ziegler, D. (1988). The oxygen electrode reaction in acid solutions on RuO2 electrodes prepared by the thermal decomposition method. *Thin Solid Films, 163*, 301-308
37. Messaoudi, B., Joiret, S., Keddam, M., & Takenouti, H. (2001). Anodic behaviour of manganese in alkaline medium. *Electrochimica Acta, 46*(16), 2487-2498
38. Michalak, F., von Rottkay, K., Richardson, T., Slack, J., & Rubin, M. (1999). Electrochromic lithium nickel oxide thin films by RF-sputtering from a LiNiO2 target. *Electrochimica Acta, 44*(18), 3085-3092
39. Mondal, S. K., & Munichandraiah, N. (2008). Anodic deposition of porous RuO2 on stainless steel for supercapacitor studies at high current densities. *Journal of Power Sources, 175*(1), 657-663
40. Pandolfo, A. G., & Hollenkamp, A. F. (2006). Carbon properties and their role in supercapacitors. *Journal of Power Sources, 157*(1), 11-27
41. Pang, S. C., Anderson, M. A., & Chapman, T. W. (2000). Novel Electrode Materials for Thin-Film Ultracapacitors: Comparison of Electrochemical Properties of Sol-Gel-Derived and Electrodeposited Manganese Dioxide. *Journal of The Electrochemical Society, 147*(2), 444-450
42. Patake, V. D., & Lokhande, C. D. (2008). Chemical synthesis of nano-porous ruthenium oxide (RuO2) thin films for supercapacitor application. *Applied Surface Science, 254*(9), 2820-2824
43. Patake, V. D., Lokhande, C. D., & Joo, O. S. (2009). Electrodeposited ruthenium oxide thin films for supercapacitor: Effect of surface treatments. *Applied Surface Science, 255*(7), 4192-4196
44. Pathan, H. M., & Lokhande, C. D. (2004). Deposition of metal chalcogenide thin films by successive ionic layer adsorption and reaction (SILAR) method. *Bulletin of Materials Science, 27*(2), 85-111
45. Patil, U. M., Kulkarni, S. B., Jamadade, V. S., & Lokhande, C. D. (2011). Chemically synthesized hydrous RuO2 thin films for supercapacitor application. *Journal of Alloys and Compounds, 509*(5), 1677-1682
46. Pei, L., Zhang, X., Zhang, L., Zhang, Y., & Xu, Y. (2016). Solvent influence on the morphology and supercapacitor performance of the nickel oxide. *Materials Letters, 162*, 238-241
47. Poizot, P., Laruelle, S., Grugeon, S., Dupont, L., & Tarascon, J. M. (2000). Nano-sized transition-metal oxides as negative-electrode materials for lithium-ion batteries. *Nature, 407*(6803), 496-499
48. Sarkar, A., Kumar Satpati, A., Kumar, V., & Kumar, S. (2015). Sol-gel synthesis of manganese oxide films and their predominant electrochemical properties. *Electrochimica Acta, 167*, 126-131
49. Sharma, P., & Bhatti, T. S. (2010). A review on electrochemical double-layer capacitors. *Energy Conversion and Management, 51*(12), 2901-2912
50. Shen, J., Li, T., Huang, W., Long, Y., Li, N., & Ye, M. (2013). One-pot polyelectrolyte assisted hydrothermal synthesis of RuO2-reduced graphene oxide nanocomposite. *Electrochimica Acta, 95*, 155-161
51. Shi, X., Zeng, Z., Guo, E., Long, X., Zhou, H., & Wang, X. (2017). A growth mechanism investigation on the anodic deposition of nanoporous gold supported manganese oxide nanostructures for high performance flexible supercapacitors. *Journal of Alloys and Compounds, 690*, 791-798

52. Singh, A. K., Sarkar, D., Karmakar, K., Mandal, K., & Khan, G. G. (2016). High-Performance Supercapacitor Electrode Based on Cobalt Oxide–Manganese Dioxide–Nickel Oxide Ternary 1D Hybrid Nanotubes. *ACS Applied Materials & Interfaces, 8*(32), 20786-20792
53. Tahmasebi, M. H., Vicenzo, A., Hashempour, M., Bestetti, M., Golozar, M. A., & Raeissi, K. (2016). Nanosized Mn-Ni oxide thin films via anodic electrodeposition: a study of the correlations between morphology, structure and capacitive behaviour. *Electrochimica Acta, 206*, 143-154
54. Toupin, M., Brousse, T., & Bélanger, D. (2004). Charge Storage Mechanism of MnO_2 Electrode Used in Aqueous Electrochemical Capacitor. *Chem. Mater., 16*(16), 3184-3190
55. Trasatti, S. (1987). Progress in the understanding of the mechanism of chlorine evolution at oxide electrodes. *Electrochimica Acta, 32*(3), 369-382
56. Trasatti, S., & Buzzanca, G. (1971). Ruthenium dioxide: A new interesting electrode material. Solid state structure and electrochemical behaviour. *Journal of Electroanalytical Chemistry and Interfacial Electrochemistry, 29*(2), A1-A5
57. Unnikrishnan, B., Wu, C.-W., Chen, I. W. P., Chang, H.-T., Lin, C.-H., & Huang, C.-C. (2016). Carbon Dot-Mediated Synthesis of Manganese Oxide Decorated Graphene Nanosheets for Supercapacitor Application. *ACS Sustainable Chemistry & Engineering, 4*(6), 3008-3016
58. Wang, C., Liu, J., Yang, Q., Sun, P., Gao, Y., Liu, F., . . . Lu, G. (2015). Ultrasensitive and low detection limit of acetone gas sensor based on W-doped NiO hierarchical nanostructure. *Sensors and Actuators B: Chemical, 220*, 59-67
59. Wang, X., Han, X., Lim, M., Singh, N., Gan, C. L., Jan, M., & Lee, P. S. (2012). Nickel Cobalt Oxide-Single Wall Carbon Nanotube Composite Material for Superior Cycling Stability and High-Performance Supercapacitor Application. *The Journal of Physical Chemistry C, 116*(23), 12448-12454
60. Wang, X., Yin, Y., Hao, C., & You, Z. (2015). A high-performance three-dimensional micro supercapacitor based on ripple-like ruthenium oxide–carbon nanotube composite films. *Carbon, 82*, 436-445
61. Wu, C.-H., Ma, J.-S., & Lu, C.-H. (2012). Synthesis and characterization of nickel–manganese oxide via the hydrothermal route for electrochemical capacitors. *Current Applied Physics, 12*(4), 1190-1194
62. Wu, X., Wang, Q., Zhang, W., Wang, Y., & Chen, W. (2016). Nano nickel oxide coated graphene/polyaniline composite film with high electrochemical performance for flexible supercapacitor. *Electrochimica Acta, 211*, 1066-1075
63. Wu, X., Xiong, W., Chen, Y., Lan, D., Pu, X., Zeng, Y., . . . Zhu, Z. (2015). High-rate supercapacitor utilizing hydrous ruthenium dioxide nanotubes. *Journal of Power Sources, 294*, 88-93
64. Wu, Z.-S., Wang, D.-W., Ren, W., Zhao, J., Zhou, G., Li, F., & Cheng, H.-M. (2010). Anchoring Hydrous RuO2 on Graphene Sheets for High-Performance Electrochemical Capacitors. *Advanced Functional Materials, 20*(20), 3595-3602
65. Xu, J., Ju, Z., Cao, J., Wang, W., Wang, C., & Chen, Z. (2016). Microwave synthesis of nitrogen-doped mesoporous carbon/nickel-cobalt hydroxide microspheres for high-performance supercapacitors. *Journal of Alloys and Compounds, 689*, 489-499
66. Xu, Y., Wang, L., Cao, P., Cai, C., Fu, Y., & Ma, X. (2016). Mesoporous composite nickel cobalt oxide/graphene oxide synthesized via a template-assistant co-precipitation route as electrode material for supercapacitors. *Journal of Power Sources, 306*, 742-752

67. Yadav, A. A., Jadhav, S. N., Chougule, D. M., Patil, P. D., Chavan, U. J., & Kolekar, Y. D. (2016). Spray deposited Hausmannite Mn3O4 thin films using aqueous/organic solvent mixture for supercapacitor applications. *Electrochimica Acta, 206*, 134-142
68. Zang, X., Sun, C., Dai, Z., Yang, J., & Dong, X. (2017). Nickel hydroxide nanosheets supported on reduced graphene oxide for high-performance supercapacitors. *Journal of Alloys and Compounds, 691*, 144-150
69. Zhang, J., Kong, L.-B., Cai, J.-J., Li, H., Luo, Y.-C., & Kang, L. (2010). Hierarchically porous nickel hydroxide/mesoporous carbon composite materials for electrochemical capacitors. *Microporous and Mesoporous Materials, 132*(1–2), 154-162
70. Zhang, J., Ma, J., Zhang, L. L., Guo, P., Jiang, J., & Zhao, X. S. (2010). Template Synthesis of Tubular Ruthenium Oxides for Supercapacitor Applications. *The Journal of Physical Chemistry C, 114*(32), 13608-13613
71. Zhang, R., Liu, J., Guo, H., & Tong, X. (2014). Hierarchically porous nickel oxide nanoflake arrays grown on carbon cloth by chemical bath deposition as superior flexible electrode for supercapacitors. *Materials Letters, 136*, 198-201
72. Zhao, B., Wang, T., Jiang, L., Zhang, K., Yuen, M. M. F., Xu, J.-B., . . . Wong, C.-P. (2016). NiO mesoporous nanowalls grown on RGO coated nickel foam as high performance electrodes for supercapacitors and biosensors. *Electrochimica Acta, 192*, 205-215
73. Zhao, D., Guo, X., Gao, Y., & Gao, F. (2012). An Electrochemical Capacitor Electrode Based on Porous Carbon Spheres Hybrided with Polyaniline and Nanoscale Ruthenium Oxide. *ACS Applied Materials & Interfaces, 4*(10), 5583-5589
74. Zhao, X., Sanchez, B. M., Dobson, P. J., & Grant, P. S. (2011). The role of nanomaterials in redox-based supercapacitors for next generation energy storage devices. *Nanoscale, 3*(3), 839-855
75. Zheng, J. P., & Jow, T. R. (1995). A New Charge Storage Mechanism for Electrochemical Capacitors. *Journal of The Electrochemical Society, 142*(1), L6-L8
76. Zhi, M., Manivannan, A., Meng, F., & Wu, N. (2012). Highly conductive electrospun carbon nanofiber/MnO2 coaxial nano-cables for high energy and power density supercapacitors. *Journal of Power Sources, 208*, 345-353
77. Zhuo, L., Wu, Y., Zhou, W., Wang, L., Yu, Y., Zhang, X., & Zhao, F. (2013). Trace Amounts of Water-Induced Distinct Growth Behaviors of NiO Nanostructures on Graphene in CO2-Expanded Ethanol and Their Applications in Lithium-Ion Batteries. *ACS Applied Materials & Interfaces, 5*(15), 7065-7071